

# A robust phase of continuous transversal gates in quantum stabilizer codes

Eric Huang,<sup>1</sup> Pierre-Gabriel Rozon,<sup>2</sup> Arpit Dua,<sup>3</sup> Sarang Gopalakrishnan,<sup>4,5</sup> and Michael J. Gullans<sup>1</sup>

<sup>1</sup>*Joint Center for Quantum Information and Computer Science,  
NIST/University of Maryland, College Park, Maryland 20742, USA.*

<sup>2</sup>*Physics Department, McGill University, Montréal, Québec H3A 2T8, Canada.*

<sup>3</sup>*Department of Physics, Virginia Tech, Blacksburg, Virginia 24061, USA.*

<sup>4</sup>*Princeton Quantum Initiative, Princeton University, Princeton, New Jersey 08540, USA.*

<sup>5</sup>*Department of Electrical and Computer Engineering,  
Princeton University, Princeton, New Jersey 08540, USA*

(Dated: October 3, 2025)

A quantum error correcting code protects encoded logical information against errors. Transversal gates are a naturally fault-tolerant way to manipulate logical qubits but cannot be universal themselves. Protocols such as magic state distillation are needed to achieve universality via measurements and postselection. A phase is a region of parameter space with smoothly varying large-scale statistical properties except at its boundaries. Here, we find a phase of continuously tunable logical unitaries for the surface code implemented by transversal operations and decoding that is robust against dephasing errors. The logical unitaries in this phase have an infidelity that is exponentially suppressed in the code distance compared to their rotation angles. We exploit this to design a simple fault-tolerant protocol for continuous-angle logical rotations. This lowers the overhead for applications requiring many small-angle rotations such as quantum simulation.

*Introduction*—Fault-tolerant quantum computing requires a universal set of fault-tolerant logical gates. Transversal unitary gates do not spread errors within code blocks so they are naturally fault-tolerant, but the Eastin-Knill theorem [1] rules out a universal set of transversal gates.

The conventional strategy for fault-tolerant non-transversal gates is to produce magic states for injection by gate teleportation [2]. This requires mid-circuit measurement and feed-forward, which has been demonstrated experimentally in linear optics [3–5], trapped ions [6, 7], superconducting circuits [8, 9], and neutral atoms [10–12]. Magic state distillation produces high fidelity magic states from many lower quality ones [13]. Numerous refinements have reduced its resource requirements [14–19], while alternative methods of growing magic states with syndrome extraction and postselection [20–22] have culminated in magic state cultivation [23–26].

Although distillation schemes may be optimized for small rotation angles [27], most protocols produce fixed-angle rotations so synthesizing arbitrary angle rotations up to some tolerance  $\epsilon$  still requires  $O(\log(1/\epsilon))$  operations [28]. This becomes costly for small rotations where we want  $\epsilon$  to be much smaller than the rotation. Thus non-distillation schemes for continuous angles based on rotations and measurements with postselection have gained interest [29, 30]. Practical limitations of near-term devices have also motivated partially fault-tolerant analog rotations [31, 32].

In this Letter, we uncover a new phase of continuous-angle logical unitaries in surface codes subjected to transversal coherent rotations [33]. We observe that these unitaries are robust against dephasing in that the applied logical unitary is known up to a logical dephasing rate  $q$

that is exponentially smaller than its logical rotation angle  $\phi$  as the code distance  $d$  increases, so that on average  $q/|\phi| \sim e^{-\kappa d}$  for some constant  $\kappa > 0$ . We apply this robustness to design a new fault-tolerant protocol that implements logical rotations using only transversal coherent rotations, syndrome measurements, and decoder-assisted corrections. We then leverage repeated rounds of these logical rotations with adaptive feed-forward to avoid postselection, resulting in an efficient fault-tolerant protocol for preparing continuously tunable small-angle magic states.

*Background*—The square rotated surface code is an  $[[n, k, d]]$  Calderbank-Shor-Steane (CSS) code which encodes  $k = 1$  logical qubit over  $n = d^2$  physical qubits for odd distance  $d \geq 3$  [34–36]. This variant of the Kitaev surface code [37, 38] has been the most popular in surface code experiments [39–44]. The qubits live on the vertices of a  $d \times d$  square grid whose faces are shaded light and dark in a checkerboard pattern, with  $X$ -type and  $Z$ -type stabilizer generators on dark and light faces respectively, as depicted in Fig. 1(c). These local checks are weight-4 in the bulk and weight-2 on the boundary. A code state can be fault-tolerantly prepared from a product state by measuring stabilizer generators and correcting or, alternatively, by using a linear-depth unitary circuit with flag qubits [45].

For storage with perfect measurements, it is resilient against dephasing up to an optimal threshold rate of  $p \approx 11\%$  [46] corresponding to the phase boundary of a random-bond Ising model. Coherent errors are systematic unitary rotations such as  $\exp(i\theta Z)$  with rotation angle  $\theta \in (-\pi/2, \pi/2]$ . Although coherent errors acting on CSS codes are difficult to analyze in general [47–49], Bravyi *et al.* [33] used a Majorana free-fermion method to estimate a threshold  $Z$ -rotation angle of  $\theta_c \approx 0.11\pi$  for

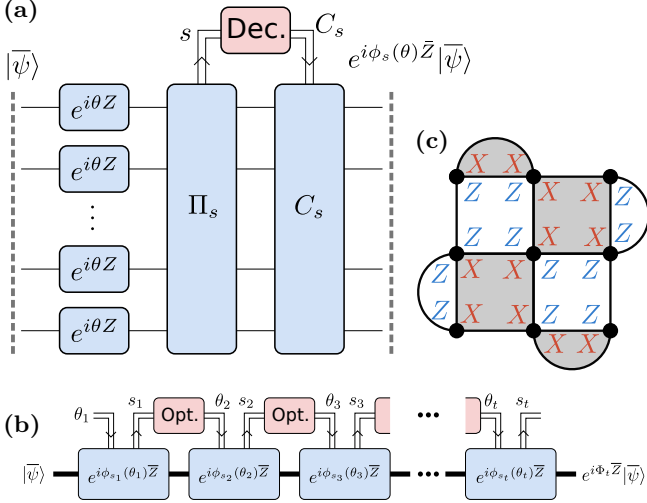


FIG. 1. (a) A CSS code state  $|\bar{\psi}\rangle$  subjected to uniform coherent  $Z$  rotations by  $\theta$ , followed by projective measurement of  $X$ -checks  $\Pi_s$  to give a syndrome  $s$  and application of the correction  $C_s$  from the decoder results in a logical channel that is a known coherent  $Z$  rotation by angle  $\phi_s(\theta)$ . (b) Repeating  $t$  rounds of coherent rotation by optimally chosen physical rotation angles  $\theta_j$  with error correction implements a potentially non-Clifford logical rotation by  $\Phi_t = \theta_1 + \dots + \theta_t$ . The classical angle optimizer (Opt.) is shaded in pink. (c) The  $d = 3$  square rotated surface code with qubits on vertices,  $X$ -checks on dark faces, and  $Z$ -checks generators on light faces.

the surface code, which has been confirmed by mappings to complex statistical mechanics models [50–53]. Applying coherent errors followed by syndrome measurement gives rise to phases of high magic [54], which motivates intentionally applying coherent rotations to produce magic states.

*Logical coherent rotation and dephasing*—Consider a round of transversal coherent rotations and decoding as shown in Fig. 1(a). A code state is transversally rotated by  $U_\theta := [\exp(i\theta Z)]^{\otimes n}$  after which a syndrome  $s$  is measured. The correction  $C_s$  from the decoder is applied, returning the system to the code space. If the CSS code has even-weight stabilizers with odd  $X$  and  $Z$  distances and  $U_\theta$  commutes with the time-reversal transformation, then the resulting logical operation is unitary [55]. These conditions are satisfied in square rotated odd-distance surface codes, resulting in a logical unitary  $\exp(i\phi_s\bar{Z})$  whose logical rotation angle  $\phi_s(\theta)$  depends only on  $\theta$  and  $s$ . More precisely, we have the identity [33]

$$\Pi_0 C_s U_\theta \Pi_0 = \sqrt{p(s)} \Pi_0 e^{i\phi_s(\theta)\bar{Z}}, \quad (1)$$

where  $\Pi_0$  is the projector onto the trivial  $X$ -syndrome,  $C_s$  is a Pauli  $Z$ -operator that produces  $X$ -syndrome  $s$  and  $p(s)$  is the syndrome measurement probability. Without noise, the applied logical angle is random but known with certainty.

When this logical rotation is repeated for  $t$  rounds, as shown in Fig. 1(b), with optimally chosen rotation angles  $\theta_j$  for each round  $j$ , then the logical rotation angles will sum to a total logical rotation angle  $\Phi_t$  which can be steered towards to a target a non-Clifford logical gate.

It thus remains to show the fault-tolerance of the protocol.  $X$  errors on the input state or before the first round of  $X$  syndrome measurements merely cause logical  $X$  errors that do not affect the logical  $Z$  angle  $\phi_s$  due to the identity in Eq. (1). The protocol can also be made fault-tolerant against measurement faults and Pauli errors that occur after the first round of syndrome measurement. To see this note that the syndrome extraction projects the state into a syndrome subspace, fixing the coherent rotation angle up to a Pauli error, so to be robust against these errors we just need to determine which syndrome subspace the system was in at the first round. This initial value of the syndrome can be learned by using  $O(d)$  rounds of conventional syndrome extraction (see Appendix) [46], or by other means [56]. On the other hand, since  $Z$  errors on the input state, or following the coherent rotation, cause syndromes from the first round of syndrome extraction that are indistinguishable from coherent  $Z$  rotations, the applied logical rotation angle is no longer knowable with certainty in the presence of  $Z$  noise. The effect of dephasing hence warrants a more careful study, which is the focus of this work.

As a general model for incoherent  $Z$  noise, we consider a round of the protocol where each qubit also suffers dephasing at a known rate  $p$  during the coherent rotations, so that each physical qubit is subjected to the channel [47]

$$\mathcal{E}(\rho) = e^{i\theta Z}[(1-p)\rho + pZ\rho Z]e^{-i\theta Z}. \quad (2)$$

After extracting a syndrome  $s$  and decoding, the logical channel will be of the same form

$$\bar{\mathcal{E}}_s(\rho) = e^{i\phi_s Z}[(1-q_s)\rho + q_s Z\rho Z]e^{-i\phi_s Z} \quad (3)$$

but with a different logical dephasing rate  $q_s$  and a logical rotation angle  $\phi_s$ . These are syndrome-dependent functions of the physical qubit channel parameters  $(p, \theta)$  and may be calculated using the tensor network method of Darmawan and Poulin [57]. The parameters will depend on the specific decoder, but in this work we use the Py-Matching decoder [58]. Although other decoders may be better-tailored to handle coherent errors [59], the results will qualitatively be the same.

The  $\theta = 0$  case corresponds to dephasing only, with the logical rotation angle  $\phi_s = 0$  for all syndromes  $s$ . In the low- $p$  and small  $\theta$  regime, the most common syndrome is the trivial syndrome  $\vec{0}$  so the  $\phi_s$  distribution is peaked the angle  $\phi_0$  corresponding to the trivial syndrome. Above the error correction threshold,  $\phi_s$  becomes almost uniformly distributed. More properties of this distribution are listed in the Appendix.

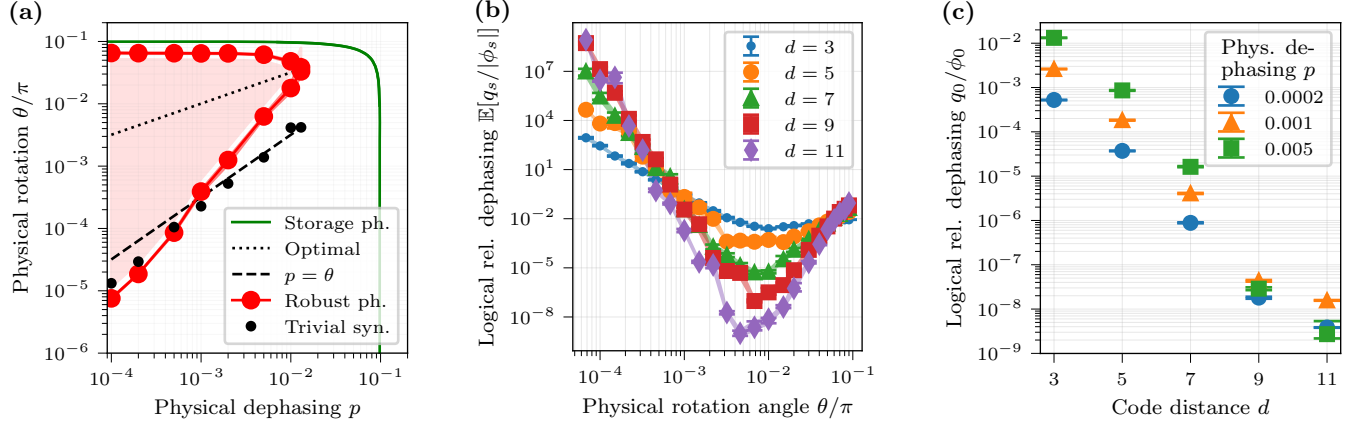


FIG. 2. (a) Phase diagram in physical channel parameter space  $(p, \theta)$ . In the robust logical coherent phase (shaded pink), the mean relative dephasing  $\mathbb{E}[q_s/|\phi_s|] \rightarrow 0$  as  $d \rightarrow \infty$  using the PyMatching decoder [58]. It is contained within the correctable phase for conventional QEC storage (shaded green) where  $\|\mathcal{E} - \mathcal{I}\|_{\diamond} \rightarrow 0$  as  $d \rightarrow \infty$ . (b) For a fixed physical dephasing  $p = 0.001$ , the mean relative dephasing has a minimum value at a  $\theta$  in the robust phase that is bounded from above and below by phase transitions. (c) The logical relative dephasing at the target angle that succeeds with 50% probability is exponentially suppressed with the distance of the code.

*Robust Phase*—In principle, a coherent rotation by a known angle  $\phi_s$  is reversible, unlike dephasing by  $q_s$ , which destroys information and increases entropy. But since each  $\phi_s$  is of a random magnitude, the logical *relative dephasing*  $q_s/|\phi_s|$  is the relevant measure of decoherence in the final state. We find evidence for the existence of a region of  $(p, \theta)$  space called the *robust phase* where the mean logical relative dephasing  $\mathbb{E}[q_s/|\phi_s|]$  over the syndrome distribution  $p(s)$  is exponentially suppressed in the thermodynamic limit  $d \rightarrow \infty$ . This phase is highlighted in Fig. 2(a) but we would expect its precise boundary to shift with a more optimal decoder. For a fixed  $p, \theta$  values in this phase are bounded from above and below by two phase transitions. The upper critical  $\theta$  beyond which recovery is impossible is expected, but the existence of a lower phase boundary where  $q_s$  dominates over  $|\phi_s|$  is novel. Within the robust phase, transversal coherent rotations and decoding lead to logical unitary rotations known to arbitrarily low infidelities.

It is well known that the regimes where quantum error correction is feasible with incoherent noise are described by ordered phases of classical statistical mechanical models, whose phase transitions correspond to thresholds [46, 60, 61]. To obtain better physical intuition for the emergence of the robust phase, we make use of a recently developed statistical mechanics mapping that can treat mixed coherent-dephasing noise channels [52, 53]. In this case, the statistical mechanics model has complex weights that account for the interference of the error terms from the coherent rotations.

The key feature of this model is that it consists of two layers of a 2D complex random bond Ising model that are coupled by a four body term arising from the incoherent noise. At low values of  $p$  and  $\theta$  the model is in a ferromagnetic phase corresponding to the below thresh-

old regime. Quenched disorder appears in the model due to the syndrome. At low-noise rates, but large values of  $p/\theta$ , the two layers of this model are locked together such that the lowest energy excited states consist of a correlated domain wall in the two layers [53]. However, as  $p/\theta \lesssim 1$ , the inter-layer coupling becomes weaker and the lowest energy excitation switches to independent domain walls in the two layers. This energy crossing in the spectrum of the statistical mechanics model is associated with the phase transition to the robust phase [see Fig. 2(a)]. The existence of this robust phase was not noticed in Ref. [53] because they used a different parameterization for the logical channel that does not readily capture the behavior of the logical relative dephasing parameter.

For sufficiently small  $\Phi_T$ , the probability of success in the first round is the probability  $p(\vec{0})$  of obtaining the trivial syndrome  $s = \vec{0}$  with  $\theta$  chosen such that  $\phi_0 = \Phi_T$ . Fig. 2(c) shows that the resulting relative dephasing  $q_0/|\phi_0|$  is suppressed exponentially with distance when exactly targeting the logical angle  $\Phi_T$  at which  $p(\vec{0}) \approx 50\%$ .

*Adaptive protocol for logical non-Clifford rotations*—The robust phase finds application in a fault-tolerant protocol for implementing non-Clifford logical gates without postselection using only transversal operations and stabilizer measurements already required for error correction.

Our protocol rotates a surface code state by a target logical  $Z$  rotation angle  $\Phi_T$ , while also being fault-tolerant against dephasing errors at a rate  $p$ . Transversally rotating all physical qubits by a carefully chosen angle  $\theta$ , measuring a syndrome  $s$  and applying the correction  $C_s$  from the decoder would result in a logical rotation angle  $\phi_s$  and logical dephasing rate  $q_s$ , both of which may be inferred from  $s, p$ , and  $\theta$ . As  $\phi_s$  may not hit the target  $\Phi_T$  on the first try, we perform more rounds until

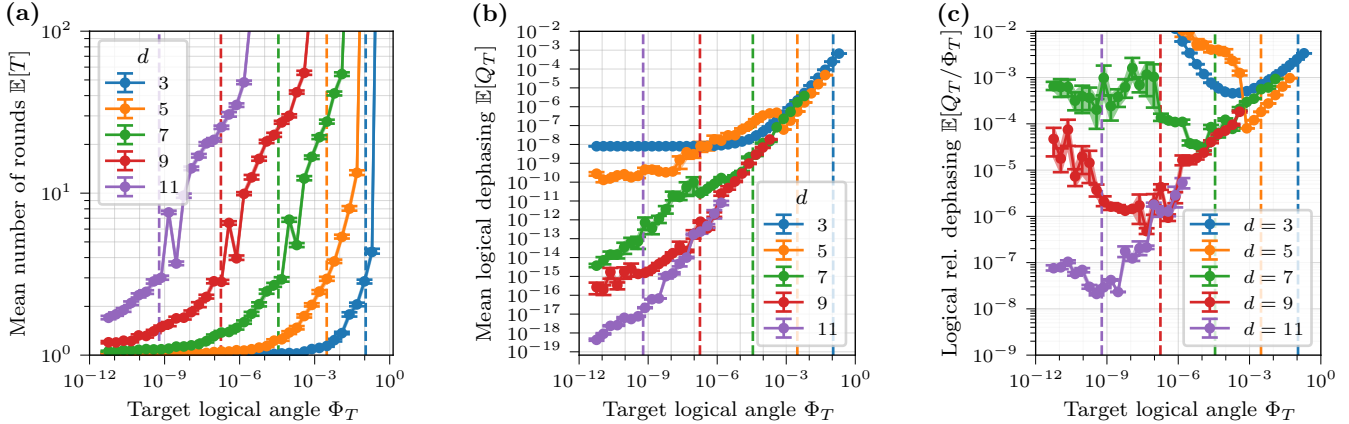


FIG. 3. Performance of the adaptive protocol with resets for preparing magic states with logical target angle  $\Phi_T$  at physical dephasing rate  $p = 0.001$ . (a) The expected number of rounds  $\mathbb{E}[T]$  including resets is independent of the tolerance  $\epsilon$ , but increases with target angle  $\Phi_T$ . (b) The total logical dephasing  $\mathbb{E}[Q_T]$  increases with the target angle  $\Phi_T$ . (c) There is a target angle where the relative logical dephasing  $\mathbb{E}[Q_T/|\Phi_T|]$  is minimal. The dashed lines indicate the target  $\Phi_T$  at which the protocol will succeed in one just round with 50% probability with the color corresponding to the code distance.

it does, tracking the total logical rotation angle  $\Phi$  and adaptively choosing  $\theta$  for each round based on a strategy that minimizes  $T$ , the number of rounds needed. This is shown in Fig. 1(b). We can also track the total logical dephasing to assess fault-tolerance, but keeping  $\theta$  in the robust phase ensures that this will be suppressed as we increase the code distance  $d$ .

The problem of choosing the best  $\theta$  is a classical stochastic control problem [62, 63]. Starting from  $\Phi_0 = 0$ , the system after  $t$  rounds of rotation is described by the total logical rotation angle  $\Phi_t$  in the ideal case. It transitions as  $\Phi_{t+1} = \Phi_t + \phi(\theta)$ , where the single-round logical rotation angle  $\phi(\theta)$  is a random variable whose distribution is parameterized by the physical rotation angle  $\theta$ , our tunable control input. For brevity we have omitted the syndrome  $s$  which is the source of randomness. The cost function to minimize  $V(\Phi)$  is the expected number of rounds  $\mathbb{E}[T]$  to reach the target  $\Phi_T$  from the present state  $\Phi$  using the optimal strategy. The policy prescribing the best input  $\theta^*(\Phi)$  for any state  $\Phi$  must satisfy the principle of optimality that the expected remaining cost to finish should equal the immediate cost  $C(\theta) = 1$  of doing one round plus the expected remaining cost from the next state. This is captured by the Bellman equation [64]

$$V(\Phi) = \min_{\theta \in (-\pi/2, \pi/2)} \mathbb{E}[C(\theta) + V(\Phi + \phi(\theta))] \quad (4)$$

for  $\Phi \neq \Phi_T$  and  $V(\Phi_T) = 0$  at the target. The best  $\theta$  would minimize the cost for each  $\Phi$ . This optimal cost function  $V(\Phi)$  may be estimated for a discretized set of  $\Phi$  values by value iteration, repeatedly evaluating the right hand side using the previous estimate to obtain a better estimate. Upon  $V(\Phi)$  converging to within numerical tolerance, the optimal policy  $\theta^*(\Phi)$  is obtained by pointwise noting the best  $\theta$  for each  $\Phi$  value.

Dephasing introduces an uncertainty of not knowing the operation actually applied, resulting in an addi-

tional logical dephasing at rate  $q(\theta)$  at each step, which accumulates to a total logical dephasing rate  $Q_{t+1} = (1 - Q_t)q(\theta) + (1 - q(\theta))Q_t$ .

Optimizing for  $\Phi_t$  to converge to a target  $\Phi_T$  without regards to  $Q_t$  will result in excessively high  $Q_t$  values. If our goal is to prepare a magic state for injection, we have the option to reset and start afresh. We can generalize the state space to  $(\Phi, Q)$  and optimize the policy similarly to minimize the total number rounds including resets. Details of the policy optimization and simulation with dephasing are in the Appendix. The expected number of rounds  $\mathbb{E}[T]$  needed to achieve the target angle  $\Phi_T$  estimated using this method is plotted in Fig. 3(a). The resulting mean total dephasing  $\mathbb{E}[Q_T]$  depends on the physical dephasing rate  $p$  and target logical angle  $\Phi_T$ . This total dephasing rate is plotted for various target angles in Fig. 3(b). We observe in Fig. 3(c) that as the code distance  $d$  increases, the mean logical relative dephasing  $\mathbb{E}[Q_T/|\Phi_T|]$  is minimized near the  $\Phi_T$  at which one round would succeed with 50% probability.

*Discussion*—In this Letter, we have shown the existence of a robust phase of continuous transversal gates in the surface code. We exploit this to introduce a low-cost adaptive protocol that efficiently implements continuously tunable fault-tolerant non-Clifford gates in the surface code over a range of rotation angles using only transversal operations and syndrome measurements. The rotation is exact and postselection was avoided with subsequent rotations and resets when preparing resource states for injection. This protocol presents a powerful new addition to the toolkit for fault-tolerant non-Clifford gates.

Our protocol is complementary to other injection ideas since it natively generates small angles which other methods struggle to achieve. However, the range of reachable logical rotation angles decreases exponentially with in-

creasing code size, which limits the applications to cases where this scaling is desirable. In particular, the protocol is more advantageous for algorithms and subroutines requiring many small rotations, such as in Trotterized quantum simulation, where the logical dephasing rate only needs to be below the truncation error [65] which depends on the step size proportional to the logical rotation angle [66]. The quantum Fourier transform [67] used for factoring [68, 69] is defined by exponentially small rotations in the input size, although these may be truncated in practice [70, 71]. Frameworks such as quantum signal processing [72] and quantum singular value transform [73] may also use many small rotations.

A natural extension of this work is to assess performance against phenomenological and circuit-level noise models using the full syndrome extraction circuits, for which we expect the results to hold qualitatively by leveraging existing fault-tolerant protocols of the surface code. It is expected that the protocol should apply for odd-distance codes satisfying the logical unitary criterion in [55], which may include more efficient quantum low-density parity check (LDPC) codes [74–77]. Further gains may be obtained by non-uniform physical qubit rotations and better decoders. Experimental demonstration of our protocol will be a future challenge.

*Acknowledgements*—We thank Kartiek Agarwal, Benjamin Béri, Matteo Ippoliti, Vedika Khemani, Chris Monroe, and Crystal Noel for helpful discussions. E.H. and M.J.G. acknowledge support from Defense Advanced Research Projects Agency (DARPA) under Agreement No. HR00112490357 and NSF QLCI award no. OMA2120757. S.G. was supported through the Co-design Center for Quantum Advantage (C2QA) under contract number DE-SC0012704. P.R. acknowledges funding support from NSERC, FRQNT and INTRIQ. EH is supported by the Fulbright Future Scholarship. This work was performed in part at the Kavli Institute for Theoretical Physics (KITP), which is supported by grant NSF PHY-2309135. We are grateful to the authors of Bravyi *et al.* [33] and Darmawan and Poulin [57] for sharing the source code for their algorithms. Simulation source code will be made available upon publication.

---

- [1] B. Eastin and E. Knill, *Physical Review Letters* **102**, 110502 (2009).
- [2] D. Gottesman and I. L. Chuang, *Nature* **402**, 390 (1999).
- [3] T. B. Pittman, B. C. Jacobs, and J. D. Franson, *Physical Review A* **66**, 052305 (2002).
- [4] R. Prevedel, P. Walther, F. Tiefenbacher, P. Böhi, R. Kaltenbaek, T. Jennewein, and A. Zeilinger, *Nature* **445**, 65 (2007).
- [5] P. Walther, K. J. Resch, T. Rudolph, E. Schenck, H. Weinfurter, V. Vedral, M. Aspelmeyer, and A. Zeilinger, *Nature* **434**, 169 (2005).

- [6] M. Riebe, H. Häffner, C. F. Roos, W. Hänsel, J. Benhelm, G. P. T. Lancaster, T. W. Körber, C. Becher, F. Schmidt-Kaler, D. F. V. James, and R. Blatt, *Nature* **429**, 734 (2004).
- [7] M. D. Barrett, J. Chiaverini, T. Schaetz, J. Britton, W. M. Itano, J. D. Jost, E. Knill, C. Langer, D. Leibfried, R. Ozeri, and D. J. Wineland, *Nature* **429**, 737 (2004).
- [8] D. Ristè, C. C. Bultink, K. W. Lehnert, and L. DiCarlo, *Physical Review Letters* **109**, 240502 (2012).
- [9] L. Steffen, Y. Salathe, M. Oppliger, P. Kurpiers, M. Baur, C. Lang, C. Eichler, G. Puebla-Hellmann, A. Fedorov, and A. Wallraff, *Nature* **500**, 319 (2013).
- [10] K. Singh, C. E. Bradley, S. Anand, V. Ramesh, R. White, and H. Bernien, *Science* **380**, 1265 (2023).
- [11] W. Huie, L. Li, N. Chen, X. Hu, Z. Jia, W. K. C. Sun, and J. P. Covey, *PRX Quantum* **4**, 030337 (2023).
- [12] D. Bluvstein, S. J. Evered, A. A. Geim, S. H. Li, H. Zhou, T. Manovitz, S. Ebadi, M. Cain, M. Kalinowski, D. Hangleiter, J. P. Bonilla Ataides, N. Maskara, I. Cong, X. Gao, P. Sales Rodriguez, T. Karolyshyn, G. Semeghini, M. J. Gullans, M. Greiner, V. Vuletić, and M. D. Lukin, *Nature* **626**, 58 (2024).
- [13] S. Bravyi and A. Kitaev, *Physical Review A* **71**, 022316 (2005).
- [14] A. M. Meier, B. Eastin, and E. Knill, *Magic-state distillation with the four-qubit code* (2012), arXiv:1204.4221 [quant-ph].
- [15] S. Bravyi and J. Haah, *Physical Review A* **86**, 052329 (2012).
- [16] P. Webster, S. D. Bartlett, and D. Poulin, *Physical Review A* **92**, 062309 (2015).
- [17] C. Gidney and A. G. Fowler, *Quantum* **3**, 135 (2019), arXiv:1812.01238 [quant-ph].
- [18] D. Litinski, *Quantum* **3**, 205 (2019).
- [19] T. Itogawa, Y. Takada, Y. Hirano, and K. Fujii, *Even more efficient magic state distillation by zero-level distillation* (2024), arXiv:2403.03991 [quant-ph].
- [20] Y. Li, *New Journal of Physics* **17**, 023037 (2015).
- [21] S. Singh, A. S. Darmawan, B. J. Brown, and S. Puri, *Physical Review A* **105**, 052410 (2022).
- [22] H. Bombín, M. Pant, S. Roberts, and K. I. Seetharam, *PRX Quantum* **5**, 010302 (2024).
- [23] C. Gidney, N. Shutty, and C. Jones, *Magic state cultivation: Growing T states as cheap as CNOT gates* (2024), arXiv:2409.17595 [quant-ph].
- [24] Y. Vaknin, S. Jacoby, A. Grimsmo, and A. Retzker, *Efficient Magic State Cultivation on the Surface Code* (2025), arXiv:2502.01743 [quant-ph].
- [25] Z.-H. Chen, M.-C. Chen, C.-Y. Lu, and J.-W. Pan, *Efficient Magic State Cultivation on  $\mathbb{RP}^2$*  (2025), arXiv:2503.18657 [quant-ph].
- [26] K. Sahay, P.-K. Tsai, K. Chang, Q. Su, T. B. Smith, S. Singh, and S. Puri, *Fold-transversal surface code cultivation* (2025), arXiv:2509.05212 [quant-ph].
- [27] E. T. Campbell and J. O’Gorman, *Quantum Science and Technology* **1**, 015007 (2016).
- [28] N. J. Ross and P. Selinger, *Optimal ancilla-free Clifford+T approximation of z-rotations* (2016), arXiv:1403.2975 [quant-ph].
- [29] H. Choi, F. T. Chong, D. Englund, and Y. Ding, *Fault Tolerant Non-Clifford State Preparation for Arbitrary Rotations* (2023), arXiv:2303.17380 [quant-ph].
- [30] Z.-C. He and Z.-Y. Xue, *High-fidelity initialization a logical qubit with multiple injections* (2025),

arXiv:2502.02897 [quant-ph].

[31] Y. Akahoshi, K. Maruyama, H. Oshima, S. Sato, and K. Fujii, *PRX Quantum* **5**, 010337 (2024).

[32] R. Toshio, Y. Akahoshi, J. Fujisaki, H. Oshima, S. Sato, and K. Fujii, Practical quantum advantage on partially fault-tolerant quantum computer (2024), arXiv:2408.14848 [cond-mat, physics:quant-ph].

[33] S. Bravyi, M. Englbrecht, R. Koenig, and N. PEARD, *npj Quantum Information* **4**, 55 (2018), arXiv:1710.02270 [quant-ph].

[34] X.-G. Wen, *Physical Review Letters* **90**, 016803 (2003).

[35] H. Bombin and M. A. Martin-Delgado, *Physical Review A* **76**, 012305 (2007).

[36] A. G. Fowler, M. Mariantoni, J. M. Martinis, and A. N. Cleland, *Physical Review A* **86**, 032324 (2012).

[37] A. Yu. Kitaev, *Annals of Physics* **303**, 2 (2003).

[38] S. B. Bravyi and A. Y. Kitaev, Quantum codes on a lattice with boundary (1998), arXiv:quant-ph/9811052.

[39] S. Krinner, N. Lacroix, A. Remm, A. Di Paolo, E. Genois, C. Leroux, C. Hellings, S. Lazar, F. Swiadek, J. Herrmann, G. J. Norris, C. K. Andersen, M. Müller, A. Blais, C. Eichler, and A. Wallraff, *Nature* **605**, 669 (2022).

[40] Y. Zhao, Y. Ye, H.-L. Huang, Y. Zhang, D. Wu, H. Guan, Q. Zhu, Z. Wei, T. He, S. Cao, F. Chen, T.-H. Chung, H. Deng, D. Fan, M. Gong, C. Guo, S. Guo, L. Han, N. Li, S. Li, Y. Li, F. Liang, J. Lin, H. Qian, H. Rong, H. Su, L. Sun, S. Wang, Y. Wu, Y. Xu, C. Ying, J. Yu, C. Zha, K. Zhang, Y.-H. Huo, C.-Y. Lu, C.-Z. Peng, X. Zhu, and J.-W. Pan, *Physical Review Letters* **129**, 030501 (2022).

[41] R. Acharya, I. Aleiner, R. Allen, T. I. Andersen, M. Ansmann, F. Arute, K. Arya, A. Asfaw, J. Atalaya, R. Babbush, D. Bacon, J. C. Bardin, J. Basso, A. Bengtsson, S. Boixo, G. Bortoli, A. Bourassa, J. Bovaird, L. Brill, M. Broughton, B. B. Buckley, D. A. Buell, T. Burger, B. Burkett, N. Bushnell, Y. Chen, Z. Chen, B. Chiaro, J. Cogan, R. Collins, P. Conner, W. Courtney, A. L. Crook, B. Curtin, S. Das, A. Davies, L. D. Lorenzo, D. M. Debroy, S. Demura, M. Devoret, A. D. Paolo, P. Donohoe, I. Drozdov, A. Dunsworth, C. Earle, T. Edlich, A. Eickbusch, A. M. Elbag, M. Elzouka, C. Erickson, L. Faoro, E. Farhi, V. S. Ferreira, L. F. Burgos, E. Forati, A. G. Fowler, B. Foxen, S. Gajjam, G. Garcia, R. Gasca, E. Genois, W. Giang, C. Gidney, D. Gilboa, R. Gosula, A. G. Dau, D. Graumann, A. Greene, J. A. Gross, S. Habegger, J. Hall, M. C. Hamilton, M. Hansen, M. P. Harrigan, S. D. Harrington, F. J. H. Heras, S. Heslin, P. Heu, O. Higgott, G. Hill, J. Hilton, G. Holland, S. Hong, H.-Y. Huang, A. Huff, W. J. Huggins, L. B. Ioffe, S. V. Isakov, J. Iveland, E. Jeffrey, Z. Jiang, C. Jones, S. Jordan, C. Joshi, P. Juhas, D. Kafri, H. Kang, A. H. Karamlou, K. Kechedzhi, J. Kelly, T. Khaire, T. Khattar, M. Khezri, S. Kim, P. V. Klimov, A. R. Klots, B. Kobrin, P. Kohli, A. N. Korotkov, F. Kostritsa, R. Kothari, B. Kozlovskii, J. M. Kreikebaum, V. D. Kurilovich, N. Lacroix, D. Landhuis, T. Lange-Dei, B. W. Langley, P. Laptev, K.-M. Lau, L. L. Guevel, J. Ledford, K. Lee, Y. D. Lensky, S. Leon, B. J. Lester, W. Y. Li, Y. Li, A. T. Lill, W. Liu, W. P. Livingston, A. Locharla, E. Lucero, D. Lundahl, A. Lunt, S. Madhuk, F. D. Malone, A. Maloney, S. Mandrá, L. S. Martin, S. Martin, O. Martin, C. Maxfield, J. R. McClean, M. McEwen, S. Meeks, A. Megrant, X. Mi, K. C. Miao, A. Mieszala, R. Molavi, S. Molina, S. Montazeri, A. Morvan, R. Movassagh, W. Mruczkiewicz, O. Naaman, M. Neeley, C. Neill, A. Nersisyan, H. Neven, M. Newman, J. H. Ng, A. Nguyen, M. Nguyen, C.-H. Ni, T. E. O'Brien, W. D. Oliver, A. Opremcak, K. Ottosson, A. Petukhov, A. Pizzuto, J. Platt, R. Potter, O. Pritchard, L. P. Pryadko, C. Quintana, G. Ramachandran, M. J. Reagor, D. M. Rhodes, G. Roberts, E. Rosenberg, E. Rosenfeld, P. Roushan, N. C. Rubin, N. Saei, D. Sank, K. Sankaragomathi, K. J. Satzinger, H. F. Schurkus, C. Schuster, A. W. Senior, M. J. Shearn, A. Shorter, N. Shutty, V. Shvarts, S. Singh, V. Sivak, J. Skrzyni, S. Small, V. Smelyanskiy, W. C. Smith, R. D. Somma, S. Springer, G. Sterling, D. Strain, J. Suchard, A. Szasz, A. Sztein, D. Thor, A. Torres, M. M. Torunbalci, A. Vaishnav, J. Vargas, S. Vdovichev, G. Vidal, B. Villalonga, C. V. Heidweiller, S. Waltman, S. X. Wang, B. Ware, K. Weber, T. White, K. Wong, B. W. K. Woo, C. Xing, Z. J. Yao, P. Yeh, B. Ying, J. Yoo, N. Yosri, G. Young, A. Zalcman, Y. Zhang, N. Zhu, and N. Zobrist, *Quantum error correction below the surface code threshold* (2024), arXiv:2408.13687.

[42] N. Berthusen, J. Dreiling, C. Foltz, J. P. Gaebler, T. M. Gatterman, D. Gresh, N. Hewitt, M. Mills, S. A. Moses, B. Neyenhuus, P. Siegfried, and D. Hayes, *Physical Re-*

view A **110**, 062413 (2024).

[44] D. Bluvstein, A. A. Geim, S. H. Li, S. J. Evered, J. P. B. Ataides, G. Baranes, A. Gu, T. Manovitz, M. Xu, M. Kalinowski, S. Majid, C. Kokail, N. Maskara, E. C. Trapp, L. M. Stewart, S. Hollerith, H. Zhou, M. J. Gullans, S. F. Yelin, M. Greiner, V. Vuletic, M. Cain, and M. D. Lukin, *Architectural mechanisms of a universal fault-tolerant quantum computer* (2025), arXiv:2506.20661 [quant-ph].

[45] R. Zen, J. Olle, L. Colmenarez, M. Puviani, M. Müller, and F. Marquardt, *Quantum Circuit Discovery for Fault-Tolerant Logical State Preparation with Reinforcement Learning* (2024), arXiv:2402.17761 [quant-ph].

[46] E. Dennis, A. Kitaev, A. Landahl, and J. Preskill, *Journal of Mathematical Physics* **43**, 4452 (2002).

[47] E. Huang, A. C. Doherty, and S. Flammia, *Physical Review A* **99**, 022313 (2019), arXiv:1805.08227 [quant-ph].

[48] J. K. Iverson and J. Preskill, *New Journal of Physics* **22**, 073066 (2020), arXiv:1912.04319 [quant-ph].

[49] Y. Suzuki, K. Fujii, and M. Koashi, *Physical Review Letters* **119**, 190503 (2017), arXiv:1703.03671 [quant-ph].

[50] J. Behrends, F. Venn, and B. Béri, *Surface codes, quantum circuits, and entanglement phases* (2022), arXiv:2212.08084 [cond-mat, physics:quant-ph].

[51] F. Venn, J. Behrends, and B. Béri, *Coherent error threshold for surface codes from Majorana delocalization* (2022), arXiv:2211.00655 [cond-mat, physics:quant-ph].

[52] J. Behrends and B. Béri, *Statistical mechanical mapping and maximum-likelihood thresholds for the surface code under generic single-qubit coherent errors* (2024), arXiv:2410.22436 [quant-ph].

[53] J. Behrends and B. Béri, *The surface code beyond Pauli channels: Logical noise coherence, information-theoretic measures, and errorfield-double phenomenology* (2025), arXiv:2412.21055 [quant-ph].

[54] P. Niroula, C. D. White, Q. Wang, S. Johri, D. Zhu, C. Monroe, C. Noel, and M. J. Gullans, *Nature Physics* **20**, 1786 (2024).

[55] Z. Cheng, E. Huang, V. Khemani, M. J. Gullans, and M. Ippoliti, *Emergent unitary designs for encoded qubits from coherent errors and syndrome measurements* (2024), arXiv:2412.04414 [quant-ph].

[56] H. Zhou, C. Zhao, M. Cain, D. Bluvstein, C. Duckering, H.-Y. Hu, S.-T. Wang, A. Kubica, and M. D. Lukin, *Algorithmic Fault Tolerance for Fast Quantum Computing* (2024), arXiv:2406.17653 [quant-ph].

[57] A. S. Darmawan and D. Poulin, *Physical Review Letters* **119**, 040502 (2017).

[58] O. Higgott and C. Gidney, *Sparse Blossom: Correcting a million errors per core second with minimum-weight matching* (2023), arXiv:2303.15933 [quant-ph].

[59] A. S. Darmawan and D. Poulin, *Physical Review E* **97**, 051302 (2018).

[60] C. Wang, J. Harrington, and J. Preskill, *Annals of Physics* **303**, 31 (2003).

[61] C. T. Chubb and S. T. Flammia, *Annales de l'Institut Henri Poincaré D* **8**, 269 (2021).

[62] D. Bertsekas, *Dynamic Programming and Optimal Control: Volume I* (Athena Scientific, 2012).

[63] M. L. Puterman, *Markov Decision Processes: Discrete Stochastic Dynamic Programming* (John Wiley & Sons, 2014).

[64] R. Bellman, *Dynamic Programming* (Dover Publications, Newburyport, 1957).

[65] S. Lloyd, *Science* **273**, 1073 (1996).

[66] A. M. Childs, Y. Su, M. C. Tran, N. Wiebe, and S. Zhu, *Physical Review X* **11**, 011020 (2021).

[67] R. Jozsa, *Proceedings of the Royal Society of London. Series A: Mathematical, Physical and Engineering Sciences* **454**, 323 (1998).

[68] P. Shor, in *Proceedings 35th Annual Symposium on Foundations of Computer Science* (1994) pp. 124–134.

[69] P. W. Shor, *SIAM Journal on Computing* **26**, 1484 (1997).

[70] D. Coppersmith, *An approximate Fourier transform useful in quantum factoring* (2002), arXiv:quant-ph/0201067.

[71] A. Barenco, A. Ekert, K.-A. Suominen, and P. Törmä, *Physical Review A* **54**, 139 (1996).

[72] G. H. Low, T. J. Yoder, and I. L. Chuang, *Physical Review X* **6**, 041067 (2016).

[73] A. Gilyén, Y. Su, G. H. Low, and N. Wiebe, in *Proceedings of the 51st Annual ACM SIGACT Symposium on Theory of Computing*, STOC 2019 (Association for Computing Machinery, New York, NY, USA, 2019) pp. 193–204.

[74] J.-P. Tillich and G. Zémor, *IEEE Transactions on Information Theory* **60**, 1193 (2014).

[75] P. Panteleev and G. Kalachev, *IEEE Transactions on Information Theory* **68**, 213 (2022).

[76] A. Leverrier and G. Zémor, in *2022 IEEE 63rd Annual Symposium on Foundations of Computer Science (FOCS)* (2022) pp. 872–883.

[77] M. B. Hastings, J. Haah, and R. O'Donnell, in *Proceedings of the 53rd Annual ACM SIGACT Symposium on Theory of Computing*, STOC 2021 (Association for Computing Machinery, New York, NY, USA, 2021) pp. 1276–1288.

[78] L. G. Valiant, in *Proceedings of the Thirty-Third Annual ACM Symposium on Theory of Computing*, STOC '01 (Association for Computing Machinery, New York, NY, USA, 2001) pp. 114–123.

[79] E. Knill, *Fermionic Linear Optics and Matchgates* (2001), arXiv:quant-ph/0108033.

[80] B. M. Terhal and D. P. DiVincenzo, *Physical Review A* **65**, 032325 (2002).

*Syndrome Sampling*—Bravyi *et al.* [33] provide an efficient algorithm to sample the syndrome distribution after single-qubit coherent rotations in an odd-distance square rotated surface code. Each surface code physical qubit is treated as the logical qubit of a *C4 code* encoded over 4 Majorana fermion modes stabilized by a single generator  $S = -c_1 c_2 c_3 c_4$ . The single-qubit Pauli operators  $X = i c_1 c_2$  and  $Z = i c_1 c_3$  become two-mode operators, while surface code stabilizer generators become products of commuting two-mode terms called *links*. Initialization, coherent rotations and measurements of these links are fermionic linear optics on Gaussian states [78–80], which are efficiently described by manipulations of a covariance matrix with only  $O(n^2)$  elements  $M_{ij} = \text{Tr}[ic_i c_j \rho]$  instead of the  $O(2^{2n})$  elements of the density matrix  $\rho$ .

We extend this to efficiently sample the syndrome distribution with both coherent rotations and dephasing. Suppose a configuration of  $Z$  errors  $Z_e$  described by an  $n$ -bit string  $e$  produces a syndrome  $H_X e$  where  $H_X$  is the  $X$ -check matrix. If the sampled syndrome with coherent rotations only is  $s$ , then  $H_X e \oplus s$  is the syndrome sampled with rotations and dephasing, where  $\oplus$  denotes bitwise addition modulo 2.

*Logical Channel Calculation*—Darmawan and Poulin [57] provide a tensor network algorithm for calculating the logical quantum channel of a rotated surface code subjected to single-qubit quantum channels on every physical qubit after measuring a given syndrome. States may be represented as a projected entangled pair state (PEPS), which places a tensor at each qubit with one physical index and virtual indices contracted against tensors of each neighbouring qubit. Operators, such as the density matrix, are represented as a projected entangled pair operator (PEPO) similar to a PEPS but with two physical indices per tensor. The projection operator for each stabilizer generator supported on up to 4 qubits is similarly represented with two physical indices per qubit tensor. To calculate the logical channel parameters via the Choi-Jamiolkowski isomorphism, they construct a Bell state  $|\Psi^+\rangle = |\bar{0}\rangle|0\rangle + |\bar{1}\rangle|1\rangle$  between the logical qubit and a perfect ancilla qubit to compute expectation values of Pauli operators. The ancilla qubit is represented as an extra physical index of the tensor on a corner qubit.

The resulting matrix elements of the Choi matrix may then be used to calculate the channel parameters in Eq. (3). We used exact contraction without truncating the bond dimensions.

*Policy Optimization with Dephasing and Reset*—When dephasing is accounted for and reset is allowed, we start from  $(\Phi, Q) = (0, 0)$  to target  $(\Phi_T, Q)$  with  $Q$  being below a maximum acceptable logical dephasing  $Q_{\text{acc}}$  of our choosing so that  $V(\Phi_T, Q) = 0$  only for  $Q \leq Q_{\text{acc}}$ . The Bellman equation for non-terminal states becomes

$$V(\Phi, Q) = \min_{\theta \in \mathcal{A}} \mathbb{E}[C(\theta) + \gamma V(f((\Phi, Q), \theta))] \quad (5)$$

where the action space  $\mathcal{A} = (-\pi/2, \pi/2] \cap \{\text{reset}\}$  also includes the option to reset at cost  $C(\text{reset}) = 1$ . We have also included a discount factor  $\gamma$  that may be less than one to speed up the convergence. The transition to the next state  $f((\Phi, Q), \theta)$  is defined by  $f((\Phi, Q), \text{reset}) = (0, 0)$  and

$$f((\Phi, Q), \theta) = (\Phi + \phi(\theta), Q + q(\theta) - 2Qq(\theta)) \quad (6)$$

for ordinary physical rotations  $\theta \in (-\pi/2, \pi/2]$ . We then solve for the optimal policy  $\theta^*(\Phi, Q)$  as previously described, discretizing the state space and using value iteration.

*Simulations with Dephasing*—We detail how the results in Fig. 3 were obtained.  $N_s = 5000$  syndromes were sampled to obtain empirical syndrome distributions  $p(s|\theta)$  for discrete  $\theta$  values in the range 0 to  $0.16\pi$ . For intermediate angles, this was linearly interpolated between those of the nearest available  $\theta$  values. The channel parameters  $\log|\phi_s(\theta)|$  and  $\log q_s(\theta)$  were linearly interpolated in  $\theta$  with signs. The policy optimization was done on this parametrized empirical distribution with the  $\Phi$  grid discretized into  $N_\Phi = 201$  log-spaced bins centered at the target  $\Phi_T$ , and the  $Q$  grid discretized into  $N_Q = 21$  log-spaced bins up to  $Q = 0.5$ . The action space was discretized into  $N_\theta = 201$  bins including reset. The value iteration was done with a discount factor of  $\gamma = 0.99$ , stopping at a cost function tolerance of  $\delta = 0.01$ . The time complexity of value iteration is  $O((N_\Phi N_Q)^2 N_\theta \log(1/\delta)/(1-\gamma))$  [62, 63]. With resets allowed, the optimization must be done for each target angle  $\Phi_T$ .

We simulated the protocol using the optimized policy for 10000 trials by resampling the interpolated empirical syndrome distribution and bootstrapping the statistics to get uncertainties, including the mean number of rounds needed including reset  $\mathbb{E}[T]$ , the mean total logical dephasing  $\mathbb{E}[Q_T]$  and the mean total relative dephasing  $\mathbb{E}[Q_T/\Phi_T]$ .

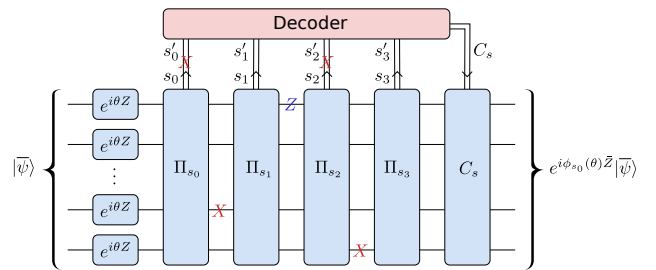


FIG. 4. Repeated rounds of measurement to tolerate measurement faults.

*Fault-tolerance*—To make our protocol tolerate measurement faults, we may use repeated rounds of syndrome extraction and decoding as shown in Fig. 4. The

key point is that generic noise after the first syndrome projection does not affect the logical  $Z$  rotation. This section of the protocol only needs to be below the usual fault-tolerant threshold for the surface code in order to reliably extract the syndrome result at the first time slice. Once this decoding process is completed, one then uses the inferred initial syndrome to compute the logical angle applied (assuming knowledge of the noise model).

*Distribution Properties*—We list some useful properties of the syndrome and logical angle distribution.

1. The syndrome probability  $p(s|\theta) = p(s|-\theta)$  is an even function of the physical rotation. This holds even with a  $Z$ -error  $Z_e$ .  $p(s|\theta, e) = p(s|-\theta, e)$ .
2. The logical angle is an odd function of the physical angle.  $\phi_s(-\theta) = -\phi_s(\theta)$ . This holds with dephas-

ing  $\phi_s(-\theta, e) = -\phi_s(\theta, e)$ .

3. Dephasing scrambles the syndrome distribution.  $p(s|\theta, e) = p(s \oplus H_x e|\theta, \vec{0})$ .
4. Dephasing scrambles logical rotation angles and causes logical dephasing dependent on the decoder. Let  $\ell_X \in \mathbb{Z}_2^n$  represent the  $\overline{X}$  logical operator and let  $D(s) \in \mathbb{Z}_2^n$  represent the  $Z$ -correction  $C_s = Z_{D(s)}$  output by the decoder for an  $X$ -syndrome  $s$ . If  $\ell_X \cdot [D(s) + e + D(H_X e)] = 0$ , then  $\phi_s(\theta, e) = \phi_{s \oplus H_X e}(\theta, 0)$  otherwise  $\phi_s(\theta, e) = \phi_{s \oplus H_X e}(\theta, 0) + \pi/2$ . All bitwise operations are modulo 2 and  $\phi_s$  is restricted to  $(-\pi/2, \pi/2]$  with periodic boundaries.